P5.27 STUDIES WITH THE CERES WINDOW CHANNEL

G. Louis Smith*
Virginia Polytechnic Institute and State University
NASA Langley Research Center
Hampton, Virginia 23681
and
Pamela E. Mlynczak
Science Applications International Corp., Hampton, Virginia

1. INTRODUCTION

The Clouds and Earth Radiant Energy System (CERES) scanning radiometer was designed for the measurement of the Earth's radiation budget (Barkstrom, 1990). It has 3 channels: a total and a shortwave channel, which are used to determine broadband outgoing longwave radiation (OLR) and reflected solar radiation, and a 8 to 12 micron window channel (Wielicki et al., 1996). Water vapor only slightly affects the 8-12 µm window channel, but it strongly affects OLR. The combination of the window channel with the broadband measurements will thus permit an improved understanding of the effects of water vapor on the radiation balance of the Earth. In this paper we examine some relations between measured OLR and window fluxes.

Figure 1 shows the spectral response of the CERES window channel. The CERES instruments were calibrated in vacuum on the ground (Lee et al., 1996). The Proto-Flight Model of CERES flew aboard the Tropical Rainfall Measuring Mission (TRMM) in an orbit of 35^o inclination which precessed through all local times every 28 days. The PFM was validated in-flight (Smith et al., 1998) to better than 1% accuracy for all channels by use of the on-board calibration system. Kratz et al. (2002) demonstrated a technique for using deep convective clouds to delineate the relation between window and total channel radiances to better than 1%.

A number of operational meteorological satellite instruments have a 10-12 µm channel and many researchers have used measurements from these instruments to infer OLR in the absence of broadband measurements. The results typically have errors of 10 to 20 W-m^{-2}. These errors are due to effects of water vapor, which influences the OLR outside the window but has little influence on the measurement in the window.

In the present paper, OLR is correlated with the window channel to provide an estimate of the OLR. Because the difference of this estimate from the OLR is due to water vapor, primarily in the mid and upper troposphere, it provides a picture of water vapor distribution. Maps of the differences are constructed using measurements from the CERES instrument aboard the TRMM, which provides geographic coverage from 40^{o}N to 40^{o}S.

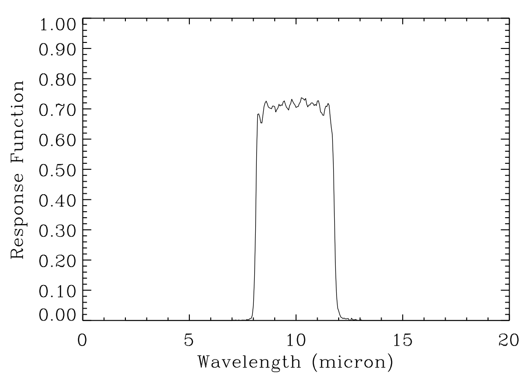

Figure 1. Spectral response of CERES 8-12 µm window channel.

2. OLR-WINDOW RELATION

Window fluxes were computed from the window radiances from the ES-8 data product (available from the Atmospheric Sciences Data Center, Langley Research Center) by use of limb-darkening functions, which were determined from CERES alongtrack data (Smith et al., 2002). Hour-box means of OLR were computed for 1^o regions covering the latitude band from 40^{o}S to 40^{o}N observed by CERES/TRMM. Figure 2 is a 2-dimensional histogram of OLR flux versus window flux for the regions viewed by CERES/TRMM in January 1998. The line through the center of the cloud of points resembles a hyperbola, thus a hyperbola was fit to the hour-box values for

**Corresponding author address*: G. Louis Smith, Mail Stop 420, Langley Research Center, NASA, Hampton, VA 23681.
e-mail: g.l.smith@larc.nasa.gov

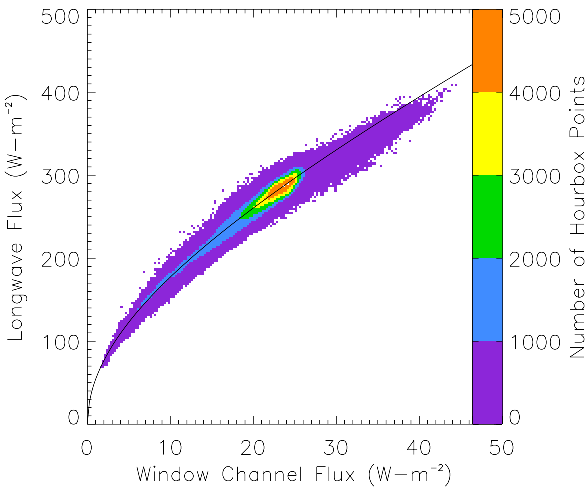

Figure 2. Histogram of OLR versus window channel flux and curve fit for all TRMM coverage area, January 1998.

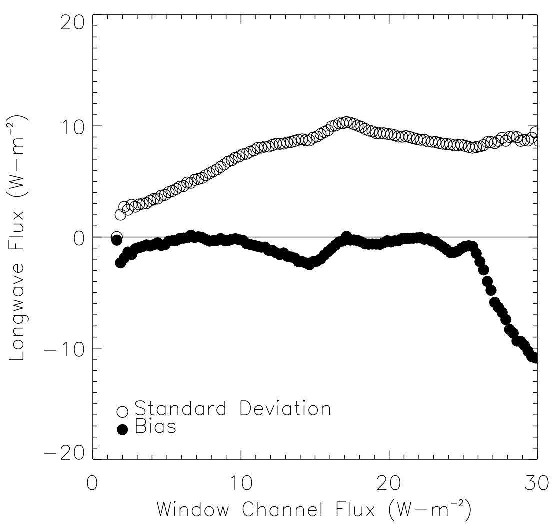

Figure 3. Bias and standard deviation of OLR derived from window channel measurements using curve fit for all TRMM coverage area, January 1998.

January and July and is shown here. Figure 3 shows the difference of OLR between the hyperbola and the centroid of the measurements, and the standard deviation of the measurements about their centroid. This standard deviation is a measure of the effect of variations of water vapor on the OLR. It is also a measure of how well one can infer OLR from the window measurement only. For window fluxes near 20 W-m^{-2}, where the histogram shows the greatest concentration of measurements, the standard deviation is on the order of 10 W-m^{-2}.

Figure 4 is a monthly-mean map of OLR as measured by the CERES broadband channels for January 1998 for the TRMM domain of 40^{o}N to 40^{o}S. A map of window flux shows substantially the same patterns though the magnitudes are quite different. Figure 5 is a map of differences of OLR minus the OLR as inferred from the window channel using the hyperbolic fit. The subsidence regions are clearly delineated by positive values of the differences and convective regions by negative values. These differences are attributed to the variations of water vapor in the mid-troposphere, which has low values in the subsidence regions and high values in convective regions. As such, this map provides information about the distribution of mid-tropospheric water vapor.

A question arises: if one selects a region with a restricted climatology, might a relation exist between OLR and window flux with a smaller variance? We try this approach over the India region.

3. OLR-WINDOW RELATION FOR INDIA REGION

The monthly-mean maps of differences appear uniform in the region of India and the nearby ocean. Assuming that mid-tropospheric water vapor has little variation or is correlated with the OLR, is it possible to compute a window to broadband relation specific to this region which will have a small error? Figure 6 is a 2-dimensional histogram of OLR flux versus window flux in January 1998 for the India region, which we define as 65^{o}E to 95^{o}E and 0^{o} to 30^{o}N. As for the global case, a hyperbola was fit to combined January and July hour-box data for the India region and is also shown in figure 6. Figure 7 shows the bias and standard deviation of the fit compared to January 1998 hour-box data. This curve fit is very similar to that for the full TRMM domain and the standard deviation is not noticeably reduced.

The curve fit for the India region was used to compute the OLR from the window fluxes and figure 8 shows the difference of this inferred OLR from the measured OLR for January 1998 for the India region. The map is dominated by differences of -5 to 10 W-m^{-2}. The errors for daily maps in the India region are not noticeably reduced from those for the entire TRMM domain. It is tentatively concluded that in the mid-troposphere water vapor amount varies greatly in this region to produce these effects on the OLR and window fluxes.

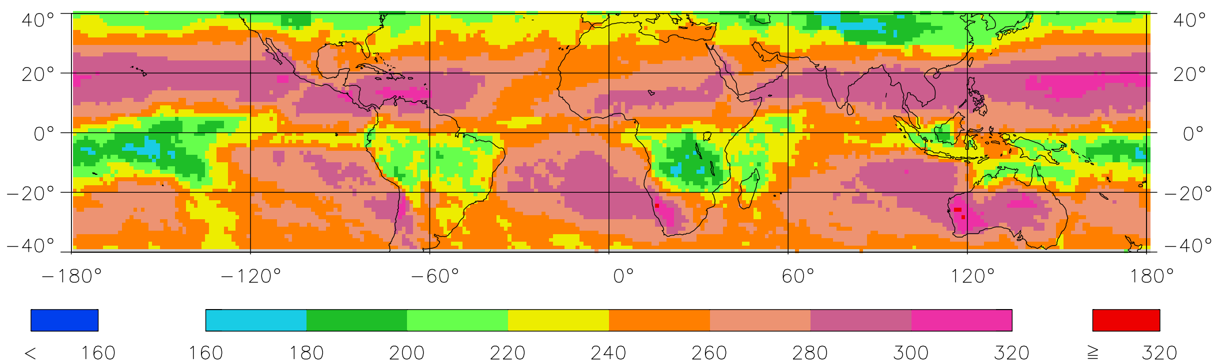

Figure 4. OLR map for January 1998, W-m^{-2}.

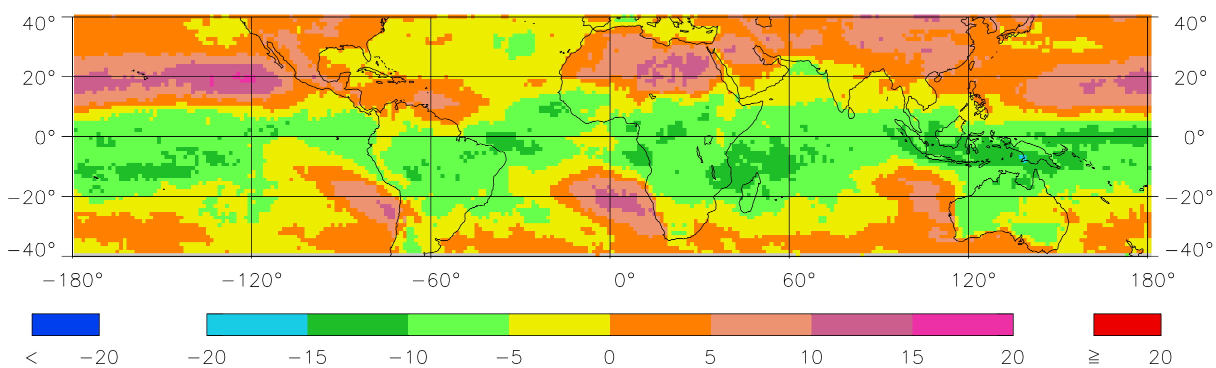

Figure 5. Map of difference between OLR as measured by broadband channels and as inferred from window channel for January 1998, W-m^{-2}.

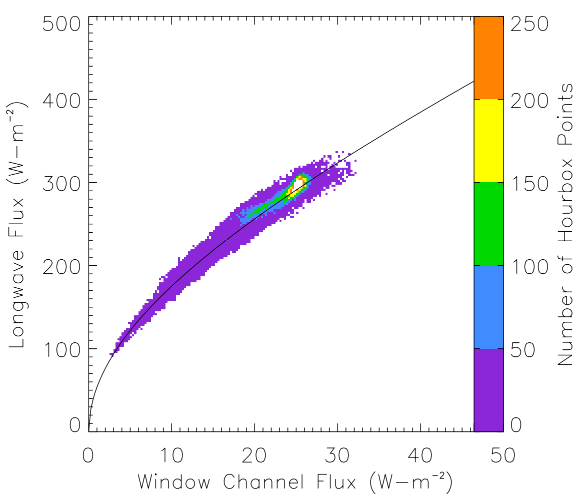

Figure 6. Histogram of OLR versus window channel flux and curve fit for India region, January 1998.

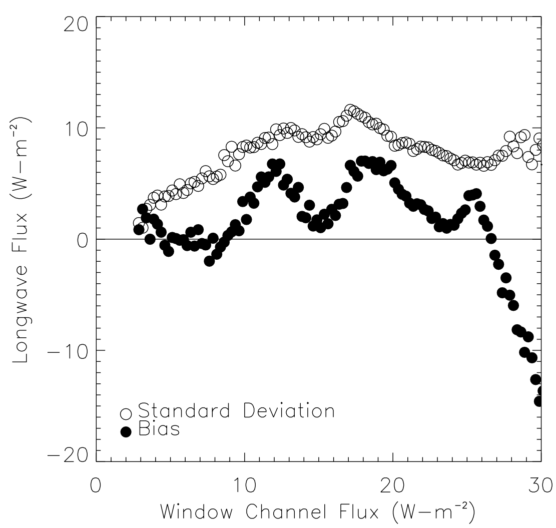

Figure 7. Bias and standard deviation of OLR derived from window channel measurements using curve fit for India region, January 1998.

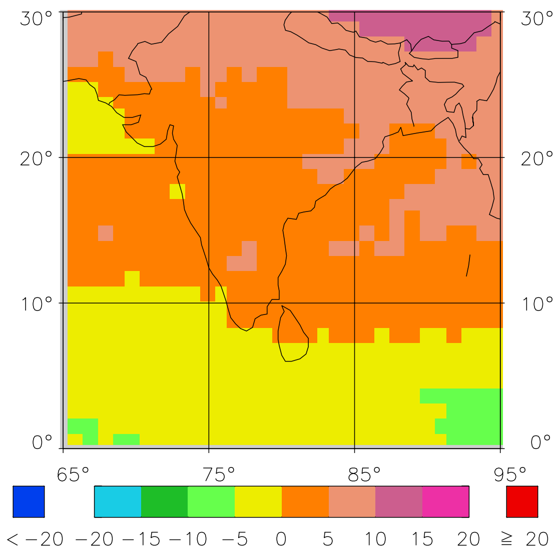

Figure 8. Map of difference between OLR as measured by broadband channels and as inferred from window channel for January 1998 for India region.

4. CONCLUDING REMARKS

In this study, maps were formed of differences between OLR and OLR inferred from window flux. These differences are largely due to variations of mid-tropospheric water vapor and contain information about its distribution. In order to understand these maps, studies using a radiative transfer model are needed to establish the relation between the vertical distribution of water vapor and these differences.

ACKNOWLEDGMENTS

This work was supported by the Earth Science Enterprise of NASA. GLS was supported through Langley Research Center by cooperative agreement with Virginia Polytechnic Institute and State University and PEM by contract with SAIC. The CERES TRMM Edition2 ES8 data were provided by the NASA Langley Research Center Atmospheric Sciences Data Center. The authors also thank Dr. David Kratz of Langley Research Center for highly useful discussions.

REFERENCES

Barkstrom, B. R., "Earth radiation budget measurements: pre-ERBE, ERBE, and CERES," *Long-Term Monitoring of the Earth's Radiation Budget,* Bruce R. Barkstrom, Ed., *Proc. SPIE,* **1299**, 52-60, 1990.

Barkstrom, B.R., B.A. Wielicki, G.L. Smith, R.B. Lee, K.J. Priestley, T.P. Charlock and D.P. Kratz, "Validation of CERES/TERRA data," *Sensors, Systems, and Next-Generation Satellites IV,* Hiroyuki Fujisada, Joan B. Lurie, Alexander Ropertz, Konradin Weber, Eds., *Proc. SPIE,* **4169**, 17-28, 2001.

Kratz, D.P., K.J. Priestley and R.N. Green, 2002: "Establishing the relationship between the CERES window and total channel measured radiances for conditions involving deep convective clouds at night," *J. Geophys. Res.,* **107**(D15), 4245, doi:10.1029/2001JD001170.

Lee, R. B. III, B. R. Barkstrom, G. L. Smith, J. E. Cooper, L. P. Kopia and R. W. Lawrence, S. Thomas, D.K. Pandey and D.H. Crommelynck, 1996: The Clouds and the Earth's Radiant Energy System (CERES) sensors and preflight calibration plans, *J. At. & O. Tech,* **13**, 300-313.

Smith, G. L., T. D. Bess, N. Manalo-Smith, V. Ramanathan, R.B. Lee, III and B.R. Barkstrom, 2002: "The CERES 8-12 μ Channel," *Adv. Space Res.,* in press.

Smith, G.L., R.B. Lee III, B.R. Barkstrom, B.A. Wielicki, K.J. Priestley, S. Thomas, J. Paden, R.S. Wilson, D.K. Pandey and K.L. Thornhill, "Overview of CERES Sensors and In-flight Performance," *Earth Observing Systems III,* William L. Barnes, Ed., *Proc. SPIE,* **3439**, 292-302, 1998.

Wielicki, B. A., B. R. Barkstrom, E. F. Harrison, R. B. Lee III, G. L. Smith and J. E. Cooper, 1996: Clouds and the Earth's Radiant Energy System (CERES): An Earth Observing System Experiment, *Bull. Amer. Met. Soc.*, **77**, 853-868.